Fiber Optics Strain Sensors

Alfredo Güemes
Dpt. Aeronautics, Univ. Politécnica de Madrid
Plaza Cardenal Cisneros, 3 MADRID 28040
SPAIN

Alfredo.guemes@upm.es

ABSTRACT

Fiber optic sensor for strain measurements, and particularly FBG (Fibre Bragg Grating) sensors, has been used for the last 20 years, and they have built up a confidence in its performances. FBGs can measure the strain with accuracy similar to the standard strain gages and extensometers, and also they are comparable in many respects from a user's point of view. Indeed, their measurements are local and directional, they require compensation for temperature, they are commonly used by bonding onto the structure surface, but also it is possible to put the optical fiber embedded in the laminate in the case of composite structures. The main advantages of the FBG over the electrical strain gage are its reliability for long term measurements, because it is frequency coded, without drifting by aging, and its ability for multiplexing, since several FBGs can be engraved on the same fiber at different positions, resulting in the simultaneous measurement points. This Chapter reviews the basic concepts, the response of free and embedded FBG sensors, and some examples of applications.

1.0 THE NATURE OF THE LIGHT

Light is commonly explained as photons that travel at the speed of the light (c_0 = 3 E8 m/s in vacuum, and c= c_0/n in a transparent medium, being n the refractive index). Light is also known to be electromagnetic waves, wavelength of visible light ranges from 400 nm (violet) to 800 nm (red).

Several theories (including mathematical models) have been done to explain the observed phenomena of the light, of increasing complexity.

Ray optics. Light satisfies the Fermat principle, it takes the minimum time to go from one point to another; consequently, it follows straight lines. This theory explains reflections and refractions.

Scalar waves. Light satisfies the Huygens equation, so the general solution is $A = A_0 \sin(\omega t + \phi)$. This theory explain the reflection, refraction, and also the diffraction, or interference phenomena (when a light beam is split in two and recombined, it may happen that the intensity drops from the original level to zero, in dependence of the differences of paths.

Electromagnetic waves. It follows the Maxwell equations. The theory explains the former phenomena, and the polarization of the light.

Quantum optics. It follows the Schrodinger equations. It is needed to explain their interaction with the matter, the absorption and emission of light.

To learn more about these theories, it is recommended the book 'Photonics', from Saleh (Ref 1). It is a marvellous book, its lecture is deeply recommended to PhD students to develop their scientific curiosity.

2.0 OPTICAL FIBRES

Fiber optic technology started in 1970's, for long distance telecommunications, and it has experienced an exponential growth during the last four decades. Sensing applications are a small spin-off from this technology, taking profit of developments done for optoelectronic components and concepts.

Optical fibers are cylindrical dielectric waveguides for the propagation of the light, made out from high purity, low loss optical materials, usually silica (Optical fibres made from plastic and other transparent materials are also commercially available, transparent at visible light). The refractive index of the core (about 1.46 for silica) is slightly higher than surrounding material or cladding, due to the presence of dopants. Light is confined at the core, because optical rays arriving to the interface core/cladding with an angle higher than the total reflectance angle, as defined by the Snell law (sen $\theta_c=n_2/n_1$), will follow total reflections and will remain confined at the core. Only when the fiber is locally bent with a sharp radius, the light may escape. The OF is externally protected from mechanical scratches with a plastic coating (the 'buffer'), and frequently several optical fibers are bundle together, and assembled with high strength mechanical fibers, such as Kevlar, to make a robust product known as optical cable, that can withstand rough industrial manipulation.

Silica optical fibers have an external diameter of 125 microns (human hair diameter range from 50 to 100 microns), and classify in two main groups.

Monomode OF, of small core (about 10 μm, depending on the intended optical wavelength). The electromagnetic waves travelling by the core must satisfy the Maxwell equations; the cylindrical contour conditions only allow for a discrete number of solutions, V, dependent on the core diameter, and the wavelength.

When $V=2\pi(a/\lambda)\ (n_1^2-n_2^2)^{1/2} < 2.4$, only one mode (2 orthogonal polarizations) propagates through the optical fiber, it is then called monomode.

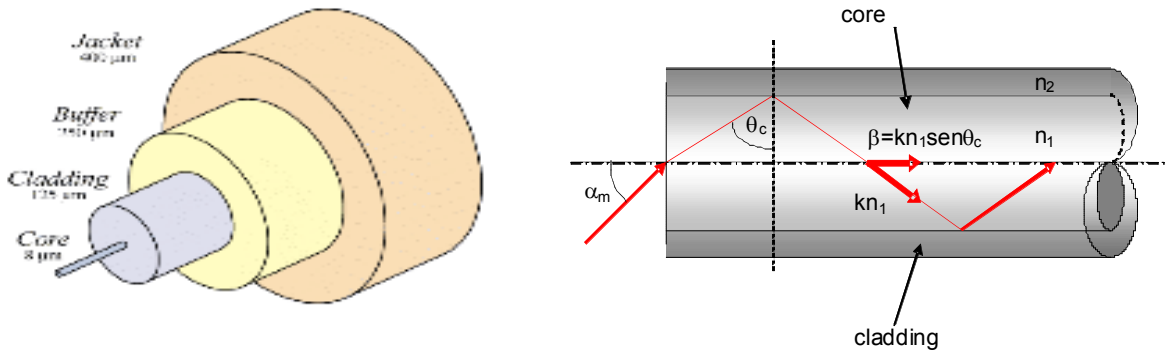

Figure 1: Representation of an optical fiber.

The multimode optical fibers have as only advantage a larger core diameter (30 to 100 microns). The larger core makes simpler the alignment with the optical sources and connections. They are preferred when used as guides for light, as in many medical applications, or in LAN. For sensing purposes they can only be used for intensity based methods.

Optical power losses (figure 2) are extremely small with current OF, in the order of 0.03 dB per kilometre, meaning that 100 km will only divide optical power by two; this is an important requirement for telecommunications. Optical power loss is minimised near the wavelengths of 1300 nm or 1550 nm., where minimum Rayleigh dispersion and minimum infrared absorption is found. From a sensing point of view,

optical losses at the fiber are irrelevant, but still 1550 nm, called C-band, is the preferred windows, because optoelectronic components are more easily available.

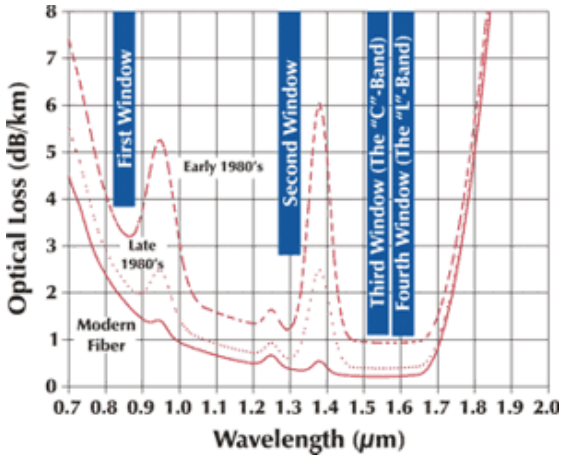

Figure 2: Attenuation of the light in the optical fibres.

NOTE on terminology:

- Decibels (dB): unit of level (relative measure). *Standard logarithmic unit for the ratio of two quantities*

X dB is $10^{-X/10}$ *in linear dimension e.g. 3 dB Attenuation =* $10^{-.3} = 0.501$.

- Decibels-milliwatt (dBm) : Decibel referenced to a milliwatt

  X mW is $10 \times \log_{10}(X)$ *in dBm, Y dBm is* $10^{Y/10}$ *in mW.*

  0 dBm=1mW, 17dBm = 50mW

3.0 CLASSIFICATION OF FIBER OPTIC SENSORS

As a wide definition, a sensor is an artifact able to transform a certain physical or chemical magnitude into readable information. Besides a topological classification (local/distributed, intrinsic/extrinsic), a more basic classification may be done by the optical parameter. Light is an electromagnetic wave, defined by its frequency, intensity, phase and polarization. The external action to be monitored must change some of the magnitudes that define the optical wave. Based on the kind of these changes, different kind of optical sensors have been developed. Nevertheless, it has to be kept in mind that direct phase measurements (display of the electrical field .VS. time) cannot be done for the optical wave, as it is done with oscilloscopes for low frequency electrical signals; only light intensity, averaging the power of the electromagnetic field, can be measured.

Our discussion will be mainly restricted to strain and temperature measurements, but fiber optic sensor may be found for many other applications (Ref 2). This would be a first classification for optical sensors, according the physical parameter sensed: chemical, mechanical, electrical, etc. Common advantages of every kind of optical fibre sensors come from its small size and weight; its non-electrical nature, making them immune to EM interference and to electrical noise, also allowing them to work into explosive environments;

they usually have a very high sensitivity and a wide operating temperature range. For Smart Structures, local intrinsic sensors are the most appreciated, because of simplicity, minimal perturbation to the host material and accuracy of reading. Multiplexing capability, or the possibility to 'write' several sensors on the same optical fiber, is another highly desired feature. A single optical fibre, 0.25 mm diameter, may afford information of strain readings from 10 to 2000 different points at the structure. When compared to the 2 leads required by each electrical strain gage, a clear advantage is found.

As illustrated at figure 3, the sketch of a fibre optic sensing system is always very simple: A solid state light source, either monochromatic (laser) or LED (light emitting diode), containing white light as a mixture of frequencies. Light goes though splices and optical connectors, used for assembly/disassembly the optical fibers, and also through couplers and circulators; a 3 dB coupler is a simple artifact where two optical fibres have been fused together, the light arriving by one end is leaving by the other opposite two ends; the couplers work identically in both directions. Light detectors use to be again solid-state, pig tailed optoelectronic components (pig tailed means that an optical fibre is leaving the solid state casing, very convenient to easily connect it to the optical circuit by a fusion splice).

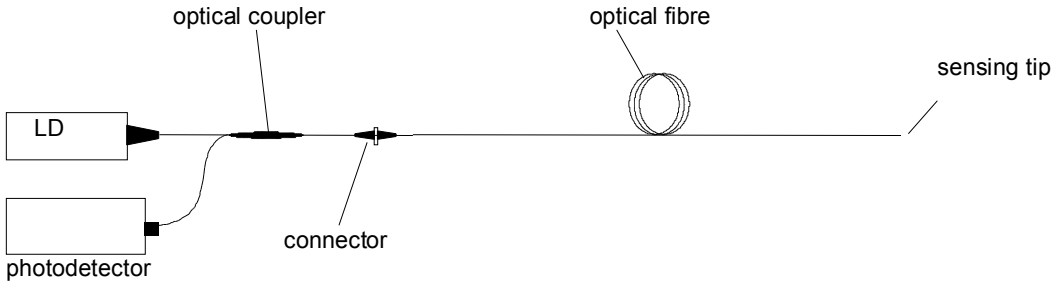

Figure 3: Sketch of a fiber optic sensing system.

3.1 Intensity-Based Sensors

These are the simplest devices among the FOS, and consequently they were among the first attempts, and still are in use as proximity sensors, for damage detection, cure monitoring and hydrogen detection. Most of the chemical sensors are of this kind. A stable light source, white or monochromatic, an optical fiber, preferably multimode for higher light power transmission and a sensitive photo detector may compose the whole system.

The amount of light reflected at the tip of the optical fiber, according the Fresnel law, is proportional to the refractive index of the external surrounding media, fig 4; this phenomena has been used for cure monitoring, (the refractive index of the resin is known to change with the cure advancement state, Ref 4), and for hydrogen leakage detection, if the tip was coated with and hydrogen sensitive material, as palladium.

$$R = \frac{(n_{core}/n_{env} - 1)^2}{(n_{core}/n_{env} + 1)^2}$$

for air $n_{core}/n_{air} = 1{,}5 \Rightarrow R = 4\%$

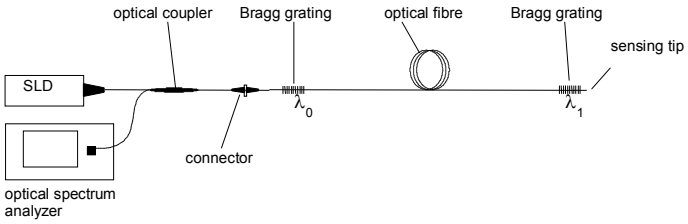

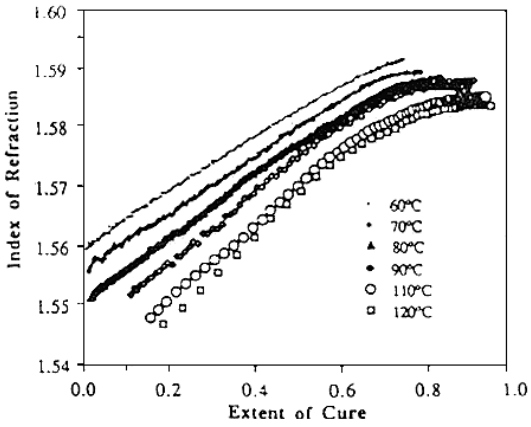

Figure 4: Sketch of cure monitoring systems by intensity based FOS.

3.2 Phase Modulated Optical Fiber Sensors, or Interferometers

Interferometry is the most accurate laboratory technique for precise distance measurements. If a continuous monochromatic light wave is divided in two beams (by a partial mirror when dealing with conventional optics, or by a coupler in the case of optical fibers), and these waves travels through different paths before being recombined, any slight difference of path-lengths will cause a delay from one wave to the other, and consequently their electromagnetic fields would not summed up, even they may counteract, and the final result is that output intensity may even cancel.

Interferometers output will move from the power input level to zero level, each time the length of any of the two paths increment or decrement in half wavelength (380 nanometers, if the red light of a He-Ne laser was used). This extreme sensitivity to any perturbation in the optical path of any of the two arms makes measurements very difficult outside the laboratory environment, because just a local temperature change may cause several maxima and minima drifting. The sensor is the whole length of the optical path of one arm, it is an 'averaging distributed sensor'. Another drawback is that measurements are related to the length when the equipment is put ON, any interruption will lose the reference; also, there is no direct indication if increment or decrement is happening, and a quadrature technique is needed to identify it.

The figure 5 sketches the most common optical fibre interferometric architectures, known as Mach-Zender, Michelson, Fabry-Perot, from the names of classical optical interferometry. At the Michelson and Fabry-Perot systems, the light is reflected at the end of the optical fibers, traveling back and recombining again. It has to be emphasized that interferometry requires monochromatic light (laser). It is very simple to arrange these optical sketches with optical fibres, all that is needed are the optoelectronic components, and one or two couplers. In spite of this simplicity, they are very seldom used. A detailed discussion of each of these systems is found at the literature. Fabry-Perot is special in the sense that light travels most of the time by a single fiber, interference is caused among the waves reflected at a partial mirror, and the waves that pass this mirror and are reflected back later. For Smart Structures, a single optical fiber was preferred, because only one ingress point into the structure is required. A lot of work was done for developing a rugged sensor head. Soldering optical fibers after partial coating of the fiber ends did intrinsic sensors. With the development of the Bragg grating sensors, this line of work was abandoned. Extrinsic Fabry-Perot heads, known as 'microcavities' are still commercially available; a precision machined wafer is bonded at the end of the optical fiber, leaving an small air gap, making miniature pressure and temperature sensors.

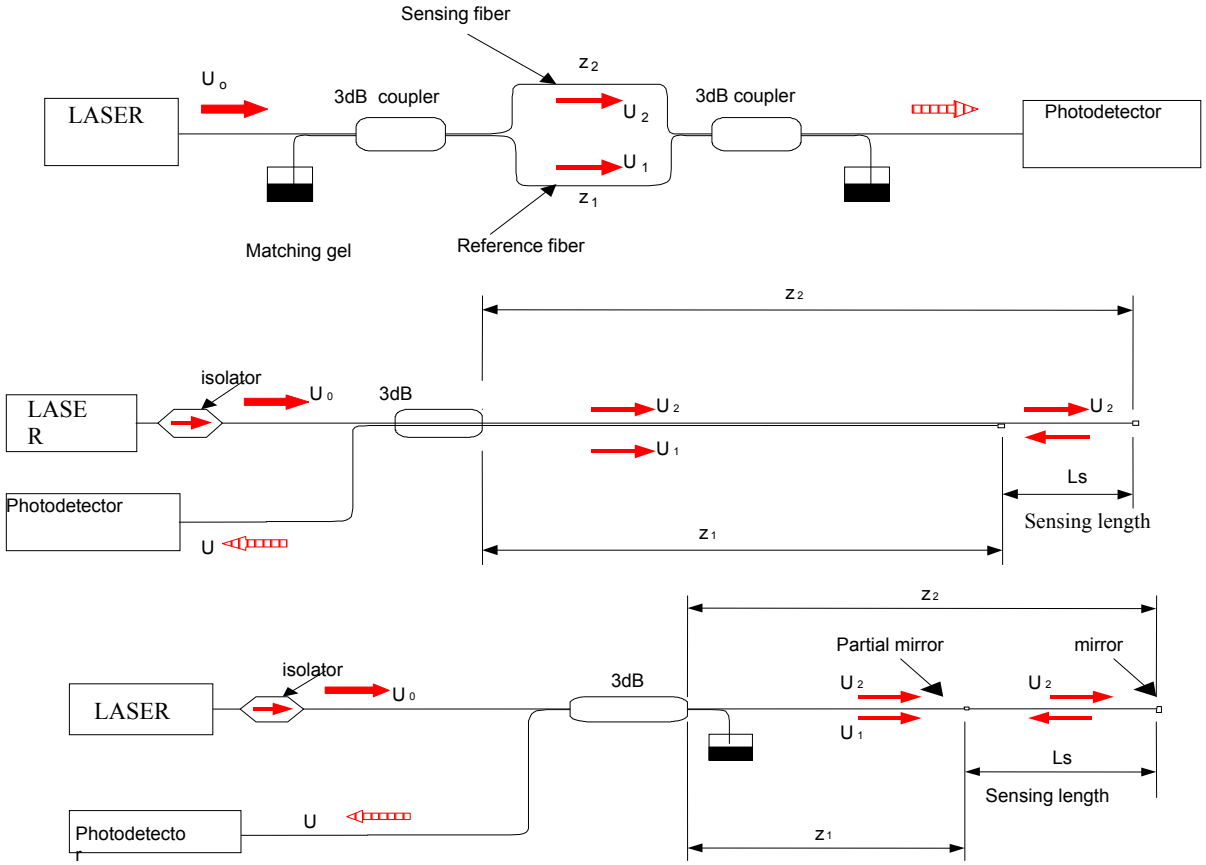

Figure 5: Typical interferometric arrangements (Mach-Zender, Michelson, Fabry-Perot).

3.3 Wavelength Based Sensors, or Bragg Gratings

These are a kind of local, intrinsic, absolute, multiplexable, interruption immune fiber optic strain sensors, which have concentrate most of the attention since its discovery, at the beginning of the 1990's.

Basic idea is to engrave, at the core of the optical fiber and for a short length (standard FBG length goes from 1 to 10 mm), a periodic modulation of its refractive index. It will behave as a set of weak partial reflecting mirrors, which by an accumulative phenomenon called diffraction will reflect back the optical wavelength that is exactly proportional to their spacing. The diffraction law, first established by Bragg and widely used for crystal structure analysis, simplifies under normal incidence to the simple expression:

$$\lambda_b = 2\overline{n_e}\Lambda_o$$

where Λ is the pitch, or period of the modulation, and n is the average refractive index. The Bragg grating behaves as a very narrow optical filter, as shown at the figure 6. When a broadband light is travelling through the fibre, the grating promotes that a very narrow wavelength band is reflected back. If the grating is subject to a uniform axial strain, or a uniform thermal increment is applied, the central wavelength of the spectrum reflected by the grating will shift due to changes in the pitch and the refractive index.

Any Optical Spectrum Analyzer (OSA) will be able to detect these changes, and transform it into readable information (figure 7).

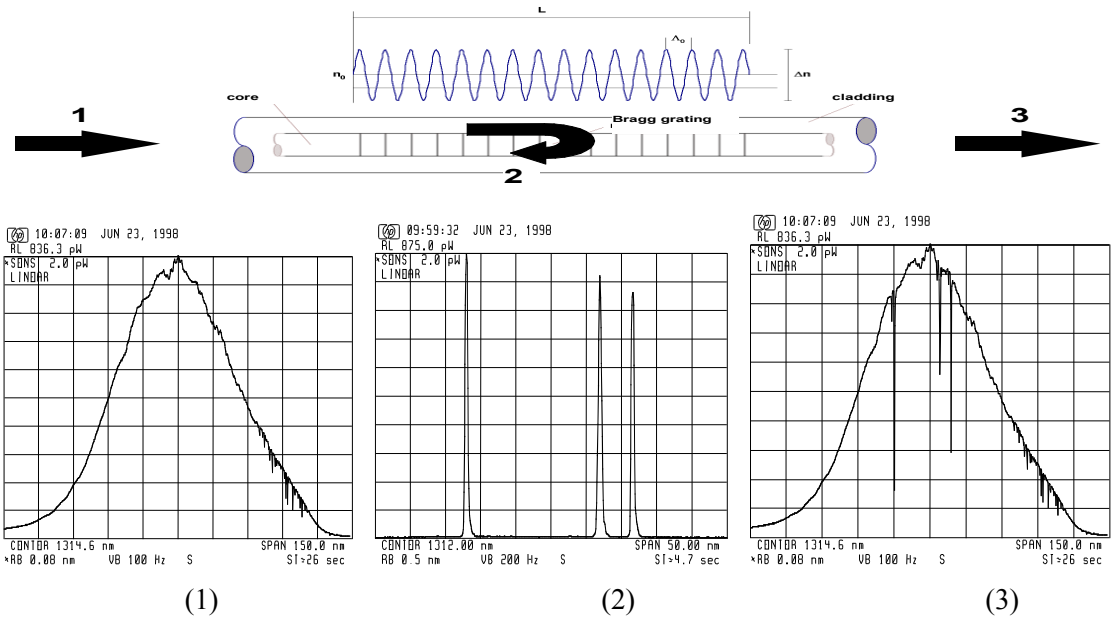

Figure 6: Fibre Bragg grating and operating principle. (1) Intensity spectrum of a broadband source launched into the fibre. (2) Spectra reflected back by three fibre Bragg gratings. (3) Transmission spectrum after passing the three Bragg gratings.

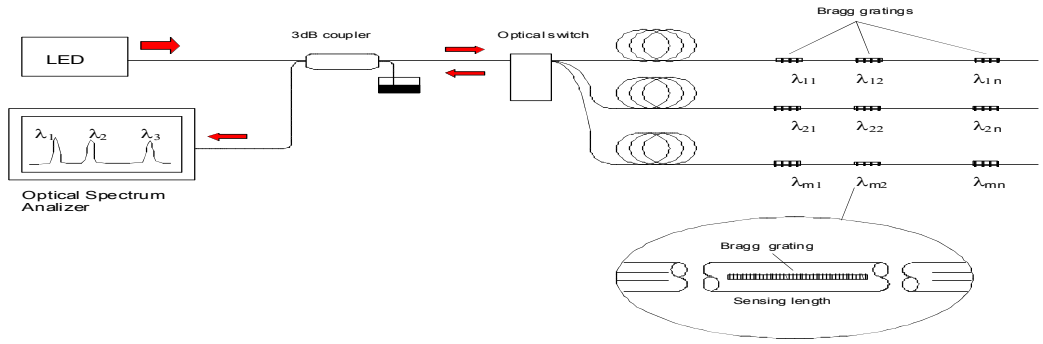

Figure 7: A multiplexed interrogation system for Bragg gratings.

Furthermore, commercially available white light sources have an spectral width around 40 to 60 nanometers. As the maximum excursion in wavelength is 10 nm for 10000 microstrains, several Bragg gratings, centered at different wavelengths, can be written at the same optical fiber, and interrogated at the same time. Multiplexing is easily implemented. The fact that the information is wavelength encoded makes the sensor very stable to aging, allowing absolute measurements of strain after long terms without recalibrating, a common nightmare with standard strain gages.

4.0 FIBRE BRAGG GRATING AS STRAIN AND TEMPERATURE SENSORS

FBG may be bought from several commercial sources, tuned at user defined central wavelength. The only ability required to the user would be to make the optical connections, normally by fusion splices, which require minor investments and training. This is the common approach for mechanical engineers, mainly interested into the usage of this technology for strain measurements. Procedures for manufacturing FBG require high investments and long trained people, and it is useful only for those people interested into the sensor development.

4.1 Response of the FBG to Uniaxial Uniform Strain Fields

When a free FBG is submitted to a uniform uniaxial tension, the photoelastic equations afford a linear relationship among the wavelength drifting and the axial strain, the proportionality coefficient is called *sensitivity factor to the axial strain:* S_ε

$$S_\varepsilon = \frac{\delta\lambda}{\varepsilon_1} = \lambda_o \left[1 - \frac{\overline{n_e}^2}{2} \left[p_{12} - \nu_f \left(p_{11} + p_{12} \right) \right] \right] \tag{3}$$

being λ_0 the wavelength for the unstrained fibre Bragg grating, $\overline{n_e}$ its refractive index, ν_f the Poisson coefficient and p_{11} y p_{12} its photoelastic coefficients. As an example, for a Bragg grating with the following parameters: Λ_o de 456.68 nm, n_e= 1,45, ν_f = 0.17, p_{11} = 0.113 y p_{12} = 0.252 it is found S= 1.04055 10^{-3} nm/με, or about 1 pm of wavelength shifting for an strain of 1 με (when the central wavelength was 1300 nm). For 1550 nm sensitivity is slightly higher, S= 1,21 pm/με.

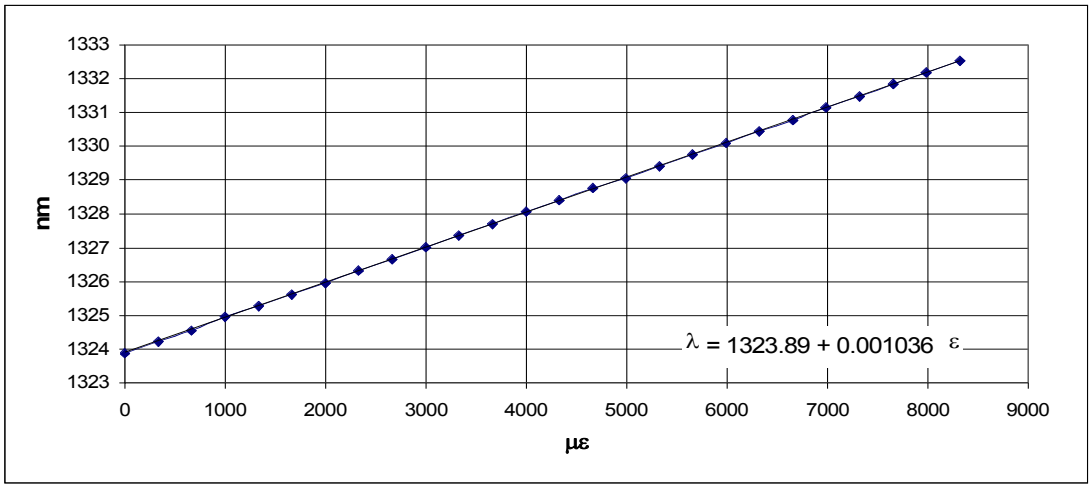

Figure 8: Wavelength shift :VS. Axial strain. FBG submitted to uniaxial strain.

Validity of this model is verified with the following experiment, with a FBG bonded on the surface of a unidirectional specimen made from graphite/epoxy AS4/8552. Results are shown at Figure 8, showing an excellent linearity and low dispersion of individual data (standard deviation: 0.01767 nm or 17.05 με). Experimentally obtained sensitivity was 1.0363.10^{-3} nm/με, quite close to those previously calculated.

4.2 Sensitivity of the FBG to Temperature

Temperature influences the behaviour of the FBG by a linear thermal expansion of the grating, and also by changes in its refractive index. Both effects may be summarized in the following expression:

$$\frac{\delta\lambda_b}{\lambda_{b,o}} = (\alpha + \zeta)\delta T \tag{4}$$

Typical values for these coefficients are. 5 to 5.5.10^{-7} for the thermal expansion of the silica, and one order of magnitude higher 8 to 10.10^{-6} for the thermo-optic coefficient. Changes in the refractive index are the main factor, and both coefficients are rather constants for a wide temperature range (-50 ºC to 500 ºC). These

values mean a drifting of about 1 nm per 100 ºC, for a grating with an unperturbed wavelength of 1300 nm. For accurate strain measurements, temperature effects need to be corrected, similarly to common strain gauges.

First exposure of the grating to high temperatures (over 100ºC) causes a partial loss of reflectivity of the grating, and also a permanent drifting in central wavelength. To get a repetitive response at high temperatures, gratings need to be annealed. Once this is done, FBG work reliably at high temperatures, up to 800 ºC.

At cryogenic conditions, for temperatures down 50 ºK, the coefficients are not longer constants, and the linearity is lost. At liquid helium (4.2 K) both coefficients are almost zero and the wavelength variation with temperature is negligible under these conditions. Special arrangements can be done to obtain accurate measurements at these very low temperatures, like bonding the sensor to a steel needle, and FBGs are very good sensors for strain and temperature at cryogenic conditions (Ref 6).

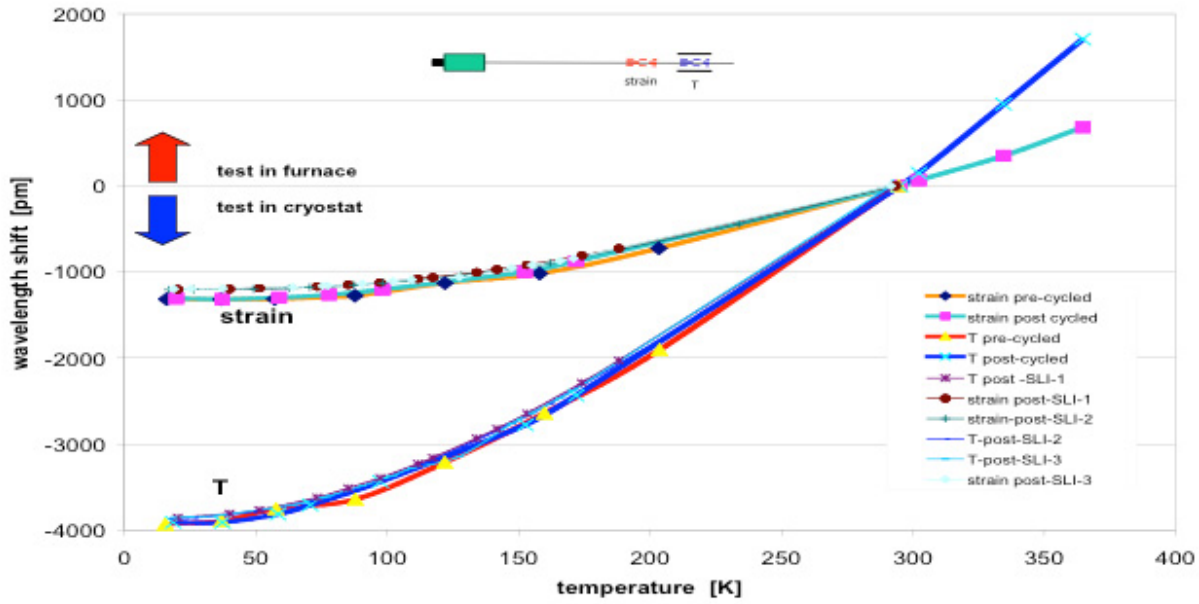

Figure 9: Wavelength shift .VS. Temperature, for a free and a steel encapsulated FBG.

4.3 Response of the FBG to Non-Uniform Uniaxial Strain Field

The reflected spectrum by an unloaded standard Bragg grating is a very narrow (0,1 nm) symmetric Gaussian peak. This spectrum may be acquired by an OSA (Optical Spectrum analyser), obtaining the optical power-wavelength. This peak would simply moves back or forwards when the BG is uniformly loaded, and its pitch, or internal periodic modulation, is changing accordingly. If the FBG would be submitted to two different strain levels along its length, two different peaks of lower height must be expected. In general terms, a strain gradient along its length will distort the reflected peak. The direct problem, or how to calculate the shape of the reflected peak corresponding to a given strain field can be easily done by the Transfer Matrix Formalism (TMF). The TMF is a numerical method to solve the coupled mode equations for aperiodic grating structures. Figure 10A shows the calculated spectra for a linear gradient, and the experimentally obtained values with a simply supported beam reproducing this strain gradient. The agreement is very acceptable.

The inverse problem, or to obtain the strain profile from the acquired spectrum, is not as straightforward, information of the intensity and phase would be required. Even some algorithms have been proposed, a simpler approach to obtain the strain gradient is to engrave several short length FBG (1mm each) as closely located as requested by the experiment. (Ref 7, 8)

This phenomena of non-uniform strains happens more often than expected. In example, if a long (10 mm) FBG is bonded on a laminate done with fabrics, a two peaks spectrum is obtained, because the strain is not uniform at the surface, the threads with parallel fibres (warp) are stiffer than transversal threads (weft). Once this behaviour is understood, it can be exploited to get more information, or avoided by embedding the sensor into a averaging material. (Ref 9)

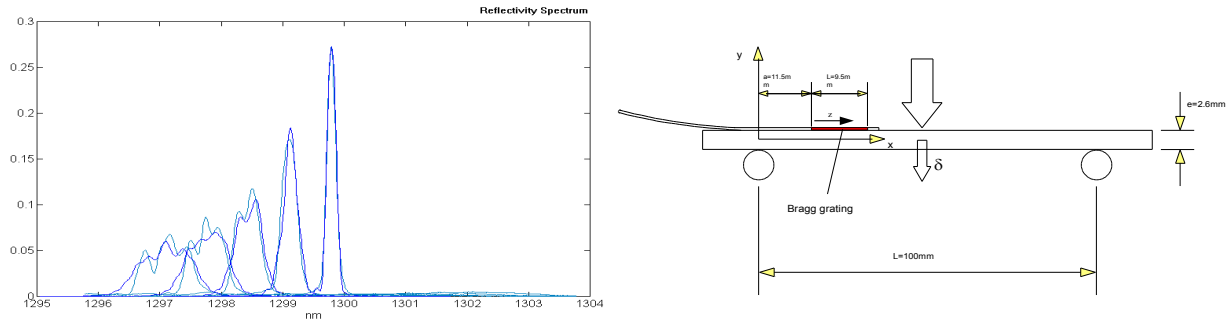

Figure 10A: Real and numerical spectra of the FBG under strain gradients; experimental arrangement.

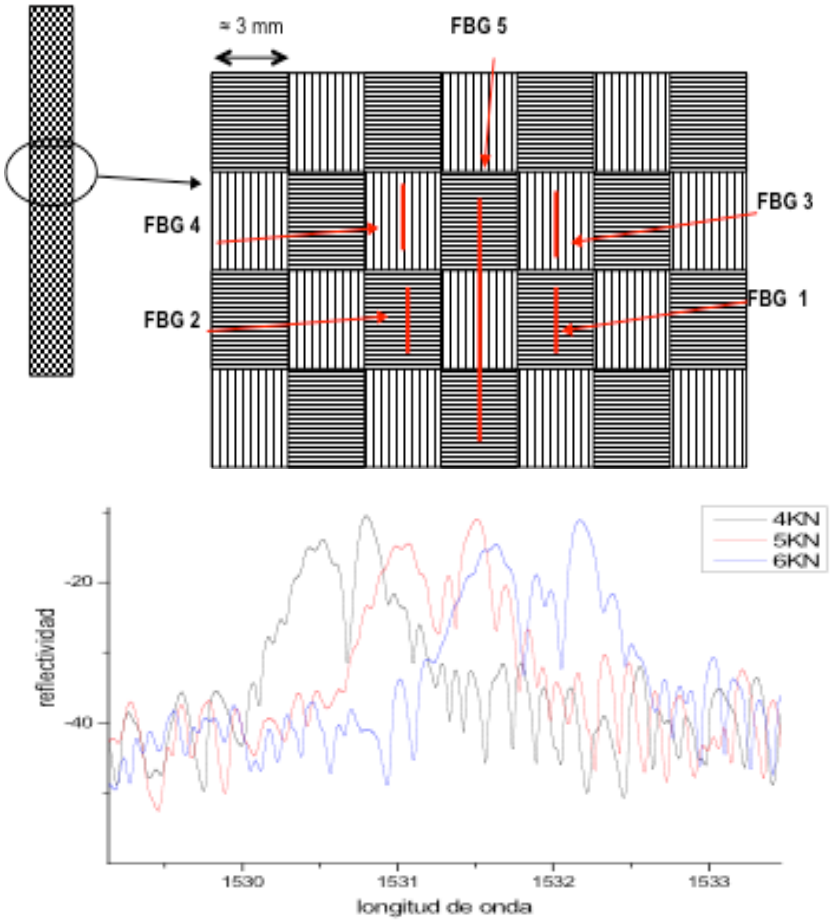

Figure 10B: FBGs bonded at the surface of a composite fabric, detecting the mesoscale strain field.

4.4 Response of the FBG to Transverse Stresses

The situation that complicates the fibre Bragg gratings is their response to non-unidirectional stresses. The first sign of this effect appears in fibre Bragg gratings embedded in a thick graphite/epoxy laminate cured at high temperature. Several gratings used to monitor strain and temperature during the cure process split in twin spectra during the cooling of the laminate. Bending of the fibre shows an exchange of optical power between the two sides of the twin spectra, pointing out a birefringence of the fibre promoted by the presence of strong residual stresses inside the laminate.

A transverse stress field applied to the grating promotes a birefringence that modifies the isotropic optical structure of the fibre, generating two principal directions of polarization, with two different refractive indexes. The fibre Bragg grating verifies two different Bragg conditions, and the optical spectrum of the grating splits in two. By using a fibre Bragg grating written in the core of a standard low-birefringence optical fibre, immersed in a general stress field, it would not be possible to separate the components of the stress field using the spectral information of the grating. Many authors have experienced these phenomena and several methods have been proposed to avoid, or minimise them: use of special fibre, encapsulate the gratings, etc.

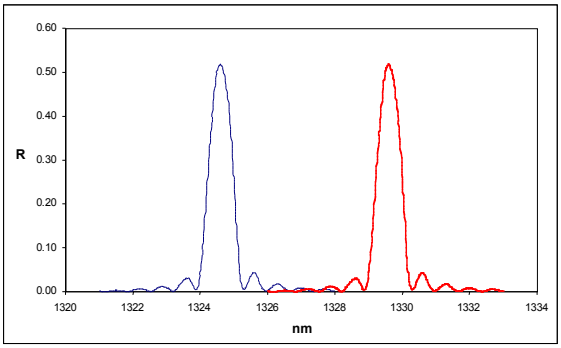

Figure 11: Spectra of a fibre Bragg grating bonded in an aluminium beam: unloaded (narrow line) and submitted to a uniform longitudinal strain of 5000 me (thick line). The "ideal" behaviour of a grating.

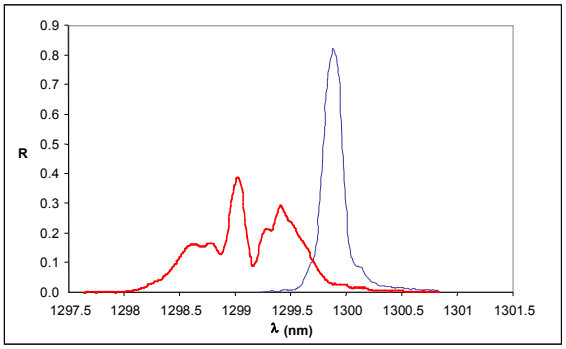

Figure 12: Spectra of a fibre Bragg grating embedded in a unidirectional composite laminate near a bonded joint: unloaded (narrow) and submitted to longitudinal load (thick). The distortion is due to strain gradients.

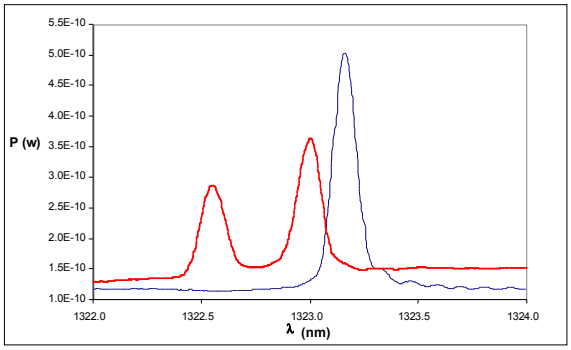

Figure 13: Spectra of a fibre Bragg grating before (narrow) and after being embedded in a thick quasi-isotropic laminate cured in autoclave (thick); the split red spectrum shows the effect of strong transverse stresses over the grating.

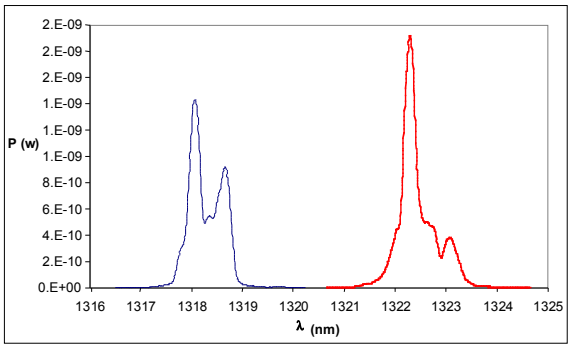

Figure 14: Spectra of a FBG embedded in a composite beam made with fabric and cured in autoclave: unloaded (narrow), shows the typical splitting of a biaxial stress state; loaded (thick), shows the effect of a complex non-uniform biaxial stress field.

Assuming an FBG submitted only to transversal stresses, a FEM analysis can be done to obtain the strains at the core in both radial directions, the two refractive indexes and the corresponding wavelength drifting. The most immediate result that can be induced is that distance between the two peaks of the splitted peak is only affected by the transverse stress applied to the fibre, and is proportional to it (figure 15), where $k \cong 70 \times 5.8514\ GPa$ is the coefficient of proportionality for a naked FBG, λ_o is the Bragg wavelength of the non-perturbed grating, and $\delta\lambda_2$ and $\delta\lambda_3$ are the wavelength shifts of the splitted peaks.

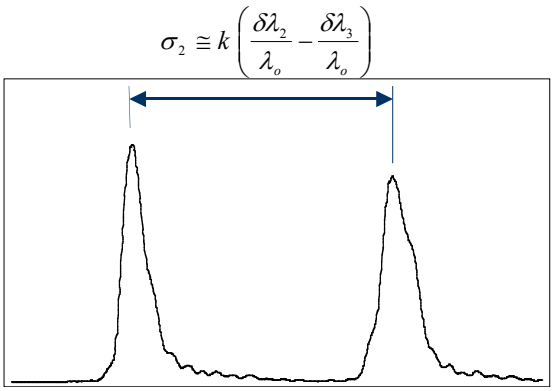

Figure 15: The distance between the two peaks of the splitted peak is only affected by the transverse stress applied to the fibre, and is proportional to it.

It is also possible to obtain an expression for the longitudinal strain of the grating as a function of the displacement of the wavelength of one of the peaks and the distance between the two peaks, $\delta\lambda = \delta\lambda_2 - \delta\lambda_3$, that is:

$$\varepsilon_1 = 1.25\frac{\delta\lambda_2}{\lambda_o} + 0.46\frac{\delta\lambda}{\lambda_o}$$

In order to prove the validity of these results, two different experimental tests have been implemented. The first one, very simple, uses the well-known thermal expansion of the aluminum to prove the importance of the effect of transverse stresses over fibre Bragg gratings in apparently very simple applications. The second test, with four gratings embedded in different positions in a graphite/epoxy laminate, will allow evaluating the effect of the residual stresses generated in a laminate during the cure process.

The use of fibre Bragg gratings to monitor strain distributions in bonded joints in aluminum elements using high temperature adhesive film was one of the first applications in which the importance of transverse stress in their spectral response appears clearly. The following test has been configured as an illustrative example of this behavior, and shows the necessary precautions that have to be taken when using this technology in applications in which temperature or external loads can promote transverse strain fields over the gratings.

Figure 16 shows a bare fibre Bragg grating 10 mm long written in photosensitive fibre and submitted to thermal stabilization at 300C during 2 hours has been bonded in a beam of AA5083 aluminum using an epoxy adhesive film. The adhesive has been cured using a standard cycle shown in the graphic of figure 17 a.

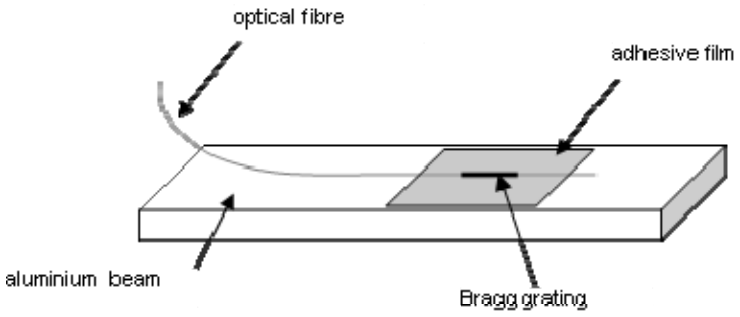

Figure 16: Schematic of aluminium beam with a fibre Bragg grating bonded using adhesive film.

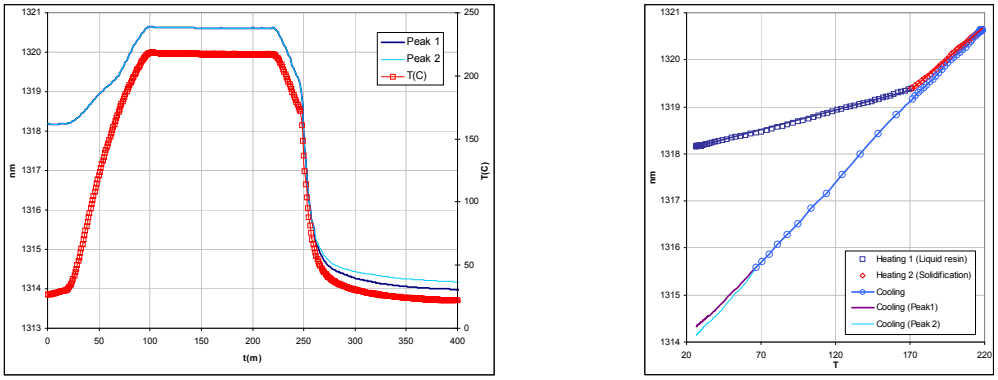

(a) (b)

Figure 17: a) Evolution of temperature and the wavelength of the Bragg wavelength of the grating during the curing cycle. The spectrum of the grating split in two during the cooling of the specimen; b) Evolution of the Bragg wavelength with temperature during the curing cycle.

Figure 17 b) shows the evolution of the Bragg wavelength of the grating with the temperature during the curing cycle. The wavelength of the grating increases during the first part of the heating stage, according the curve wavelength/temperature of a free grating, as a single peak.

At 170 ºC, there is a discontinuity in the slope promoted by the fast gelification of the resin, which forces the grating to follow the thermal expansion of the specimen. During the cooling, the wavelength decreases with this last slope, but the grating split in two at 70C (the discrimination of two different peaks depends on the resolution of the spectral analyzer used) due to the thermal transverse strain of the beam.

The wavelength shift of a grating bonded to an aluminium specimen with a linear expansion coefficient α_{Al} is given by:

$$\delta\lambda_b = \delta\lambda_{bT} + \lambda_{bo}\left(\alpha_{Al} - \alpha_f\right)\delta T$$

where $\delta\lambda_{bT}$ is the wavelength shift of the free Bragg grating with the temperature, and α_f is the linear expansion coefficient of the optical fibre. The values of linear expansion coefficient for the AA5083 aluminium and the optical fibre are known ($\alpha_{Al} = 23.5\times10^{-6}K^{-1}$ and $\alpha_f = 5.5\times10^{-7}K^{-1}$), then the value calculated for the final Bragg wavelength of the grating after the cooling is 1314.20 nm, whereas the empirical result obtained was 1314.19 nm for a cooling from 180C to 20C, demonstrating the accuracy of the model.

In this case, it is difficult to find an immediate quantitative relationship between the transverse shrinkage of the aluminium specimen and the shift of the spectrum of the grating due to the complex host/adhesive/sensor interaction.

A graphite-epoxy laminate specimen made of 24 plies of unidirectional T300/F155 prepreg tape with the following configuration: $\mathbf{[[90]_8[0]_4]_s}$, 150 × 125 × 8 mm, cured in a hot plates press at 180C in an quasi-isothermal cycle (the specimen was introduced in the press with the plates at the curing temperature. Four bare fibre Bragg gratings were embedded in the laminate parallel to the reinforcing fibres, two in the middle plane (gratings 1 and 2) and two in the outer laminae (gratings 3 and 4). Spectra of the four gratings at different stages of the process are shown in figure 18.

With these data, and using the expressions obtained from the photoelastic model, the following values of strains and stresses are calculated:

Table 1: Residual strains and stresses calculated using the photo elastic model.

Grating n°	σ_{1f} (Mpa)	σ_{2f} (Mpa)	ε_{1f}	ε_{2f}
1	-15	71	-385	1057
2	-19	78	-453	1155
3	13	84	-20	1167
4	24	50	-87	705

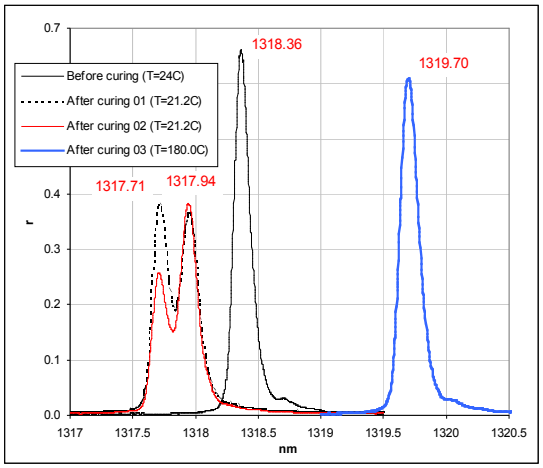

(1)

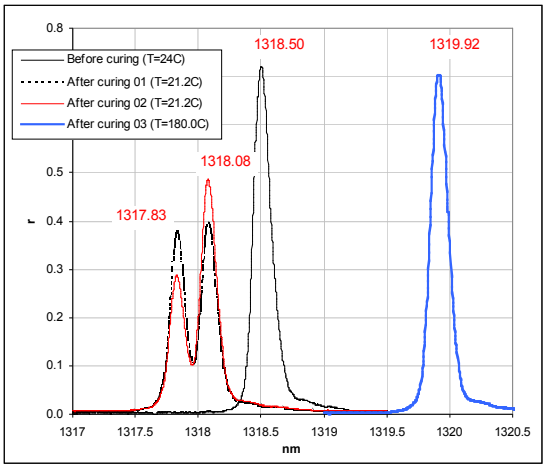

(2)

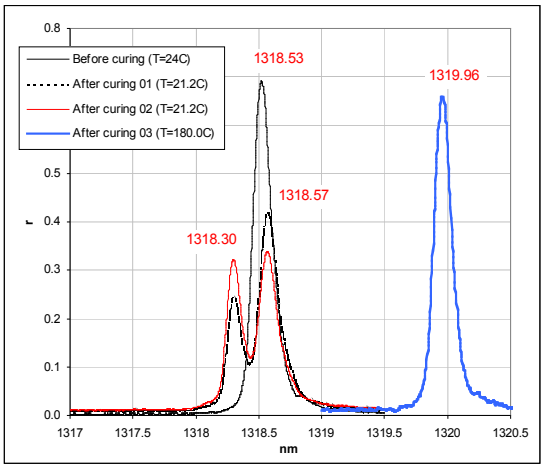

(3)

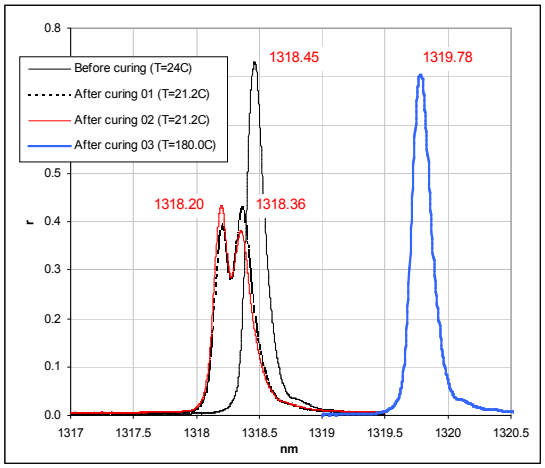

(4)

Figure 18: Spectra of the four gratings in different moments of the process: grating at 24C before curing, grating at 180C after curing (still single peak), and grating at 21.2C after curing (two peaks).

where an *"f"* has been added as a subscript to remark than these results are the strains and stresses at the core of the grating. Strains in the laminate and the optical fibre should be roughly the same, but the agreement in this case is only qualitative for the transverse direction, and how to use FBG to obtain internal residual stresses in composite laminates is still an interesting research topic. The most common approach, to avoid these complexities, is to cover the FBG with some coating that dampen the transverse stresses, reducing or eliminating the peak splitting.

4.5 Commercial FBG Interrogation Systems

The interrogation scheme given at figure 7, using an OSA (Optical Spectrum Analyzer), is too slow and bulky for practical applications; besides it, getting the detailed spectrum is not usually required, information of the peaks wavelength is enough for most of the practical cases.

FBG interrogation methods are classified by the measurement principle, which is related to the scanning frequency. Conventional systems use wavelength sweeping by mechanical moving parts by piezoelectric actuators, such as a tunable laser source or a tunable Fabry-Perot filter; they are used for the wavelength interrogation with the measurement frequency under 2 kHz, which is enough for most of the common mechanical applications. Systems based on tunable lasers are the most widely used and the most recommended for general purpose applications, combining accuracy and performances at reasonable costs.

For the measurement frequency over 1 kHz, which is required for strain measurements under impact conditions, or for the analysis of elastic waves generated into the structure, Bragg wavelength shifts should be converted into optical power through a certain type of optical filter without introducing any mechanical moving parts. A very simple and economic solution is obtained by a diffractive grating associated to a CCD array, even the resolution is not as good as with the former techniques.

The higher speed is obtained by using wavelength dependent filters, as a LPG or a AWG, being able to reach 1 Mhz, as the only limit is the speed of the photo detector. In these cases, the sensing FBG must have a wavelength centered at the window of the filter, and the span is limited to the window width; these conditions limits severely the multiplexing capability, usually based on different central wavelengths.

Recently, the company 4DSP has launched to the market a new system, working on the OFDR approach for multiplexing (based on NASA's revolutionary and patented technology), able to work with thousands of strain or temperature sensors constantly monitored up to 100 times per second. The technology will be discussed on the next Chapter on Distributed Sensing. Such a dense sensor network is required for shape sensing and damage detection applications. Current cost of the equipment is ten times higher than conventional systems.

Just below a non exhaustive list of commercial suppliers is given. Many of them include at their websites good introductions to the FBGs technology and references.

- **Tunable Laser:** Micron Optics, FiberPro, FOS SA, LiComm, Luna Innovations, OE-Land, Precision Photonics, Sabeus, Weatherford
- **Scanning Fabry-Perot filter** Axsun, WellTech, FOS&S
- **Wavelength sensitive filters** AOS, A-TEK, BRR, FiberSensing, NP-Photonics, IFOS, Technobis
- **TDM** Insensys, Technobis
- **Interferometer** R&D (non-commercial)
- **Polychromator** Ando, BaySpec, Ibsen, XenICs, Yokogawa, IPHT/Jenoptik

5.0 STRUCTURES WITH EMBEDDED FIBRE BRAGG GRATINGS

The possibilities of structural integration do not only depend on the sensor characteristics. The structural material, from now onwards denominate *host*, also have to fulfill a set of requirements to allow the integration of fibre Bragg gratings, without disturbing the manufacturing process. Host has to be immune to the presence of the optical fibre, so that its mechanical properties or its structural integrity is not modified. Because of the low size of the optical fibre, it has been verified by many authors that OF does not change the static or fatigue strength of composites, and do not act as crack initiator, if adequately oriented.

Although the fibre optic, and therefore the sensors, can be bonded externally to any material on any structure, the concept of Smart Structure carries inherently the concept of integration. Some of the advantages associated to embedding fibre optic sensors are:

- Increased survival possibilities of the optical fibre and integrated sensors, intrinsically brittle; optical fibre would be protected by the external structure.
- The existence of an intimate sensor/host union.
- The absence of external wiring, important not only from the aesthetic point of view, but also allowing its use for applications that require clean surfaces, as it is the case of aeronautical structures.
- The possibility for internal monitoring of the structure, in places which cannot be reached by conventional sensors, or would be too intrusive by their size and by the high number of wires that usually are necessary to route until them.

A full integration of sensors into the host material is limited by the material nature and by the manufacturing processes. For example, the maximum temperature for silica fibre (without external shell) is about 900ºC, limiting its possibility for embedding in metals and metal matrix composites. Concrete structures, and advanced composite materials with polymeric matrix are more adequate for integration purposes.

Manufacturing process of structural elements also limits the use of embedded fibre optics, because it is necessary to avoid potentially aggressive operations, such as high pressures application, shear stresses and very small chamfers. Another critical factor is the survival of fibre terminals to connect structural elements each other, for the output monitoring systems.

For using fibre Bragg grating as strain sensors it is necessary to have the maximum information possible about its surroundings in order to establish basic criteria to guarantee the accuracy, repeatability and stability of the measurements.

The main mission of the coating is the mechanical and environmental protection. Commonly used materials for coating optical fibre are polymers, acrylate or poliimide. The coating characteristics are also very important because the stress and strain transmission from the structural element to the fibre is made through it, and its characteristics will impose the response of the sensor/structural element. Standard optical fibre has an acrylate coating, with low elastic module, low bare strength, oxidizing at temperatures used for curing composite materials (around 180ºC). Polyimides have greater rigidity and bare strength, and do not degrade to these temperatures, reason why it is preferred for embedding in composite materials.

Some factors influencing the response are:

- The coating thickness: It has to be sufficient to isolate from transversal stresses, but not excessive, since it could be intrusive and could delay the transmission of longitudinal deformations.
- Its tolerance to the adhesive cure process or the matrix in which the fibre is embedded, decreasing its degradation to high pressures and temperatures.

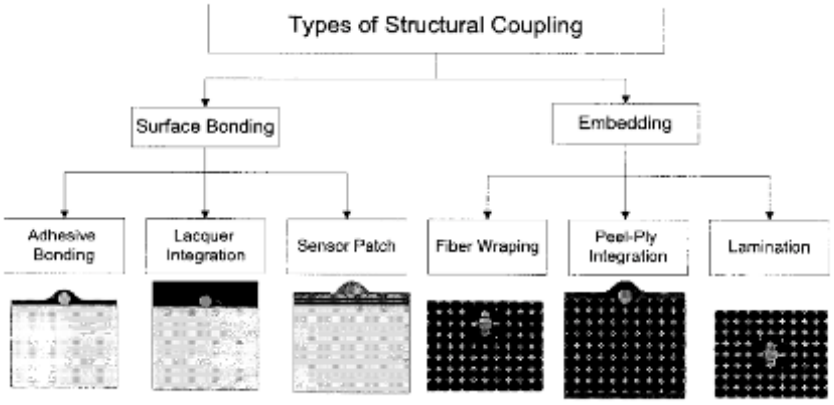

Figure 19: Representation of several ways to attach the optical fibre into the structure.

5.1 Orientation of the Optical Fibre Respective to the Reinforcement Fibers

The main factor in the behavior of fibre/host is, for the case of composite materials with long fibre reinforcement, the orientation of the optical fibre respective to the reinforcement. The monomode fibre used in Bragg grating sensors is 125 μm diameter, approximately the same thickness as a composite material lamina. In the surroundings of the optical fibre, a resin-rich zone appears, named resin pocket. (figure 20). In weave laminates the determination of resin pocket geometry is very difficult, by the complexity of the phenomena implied in its formation. In the case of tape laminates, resin pocket size is reduced when the optical fibre/ reinforcement fibre angle is reduced, and disappears when it is embedded longitudinally to them.

The resin pocket geometry and size depends on the reinforcement fibres orientation of adjacent sheets to optical fibre. The best configuration is optical fibre embedded parallel to the reinforcing fibres. In this way the resin pocket size is null, and the optical fibre interference with the laminate is practically null. It will be necessary to set reduced points in which the angle optical fibre/reinforcement is not null and identify them as possible sensitive zones.

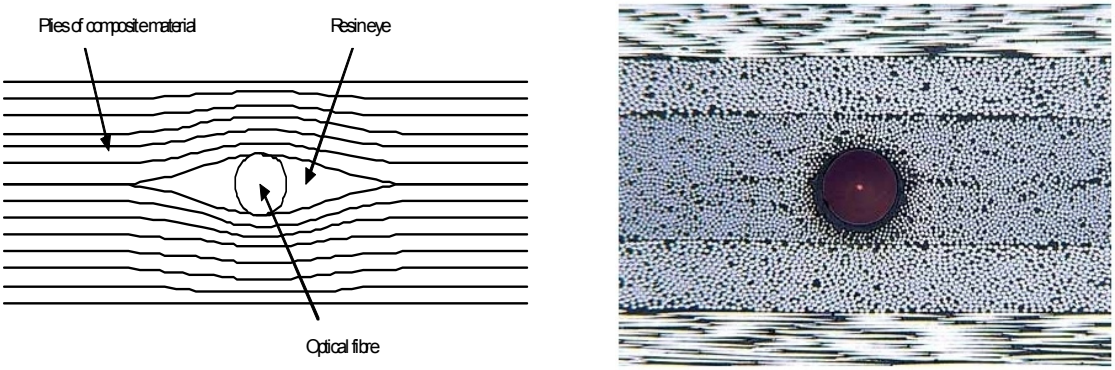

Figure 20: Sketch of the laminate cross section, showing the 'resin eye'. On the right side, an optical fibre embedded parallel to the graphite fibres of a tape laminate.

It is evident that the resin pocket, besides to create a laminate zone without reinforcement material, causes a distortion of the stresses field which may initiate a delamination process.

In laminates made with fabrics, the fibre weft, added to the applied pressure during the curing process and the differential contraction that appears during cooling may cause a fibre breakage or, if the fibre has survived the application of pressure, the build-up of a complex stresses fields and residual strain around the Bragg grating, making very difficult to analyze its response. After a lot of tests on integration of Bragg gratings in materials we concluded that best way to use Bragg gratings in this type of laminates is surface bonding or embedded between unidirectional tapes that protect the optical fibre.

5.2 Ingress/Egress from the Laminate

The input/output ends of the fibre are considered critical points for mechanical interference of the optical fibre with the structural host element. Standard procedures for input/output of the optical fiber from the composite materials still do not exist. It is due to the difficulty to edge machining the composite materials parts with optical fibre terminals or connectors leaving the laminates edges. The developments carried out during the last decade aim at two possibilities:

Use of composite materials manufacturing techniques that avoid the need of later edge trimming (RTM, SMC, RIM,…,) and would allow semi-embedded connectors on any surface of a laminate. Their effect on the mechanical behaviour of the part, and therefore the precautions to take from a point of view of the fibre survival, will be similar to conventional rigid inserts.

Output by means of pig-tails through the laminate flat surfaces, which obviously do not require any later manipulation. The effect on the laminate characteristics will depend on several factors: laminate configuration in the surroundings of the output, size and rigidity of the cable, etc.. The existence of a low module inclusion in a contour piece zone is not an optimal solution for high structural requirements applications, mainly in aeronautical applications, reason why it would have to be restricted to light loaded elements or laboratory applications. In the case of outputs by rigid inserts, the precautions to be taken will be the adapted to these kind of elements.

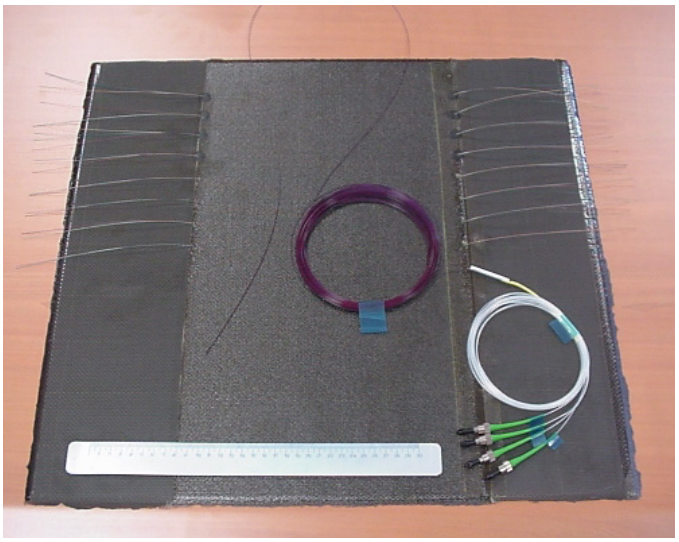

Figure 21: Cured laminate with embedded optical fibres.

6.0 APPLICATIONS IN AERONAUTIC STRUCTURES

Although not still incorporated to serial production, neither accepted for Certification procedures, a large number of demonstrations can be found in the open literature. The practical details for the implementation of

two structural elements instrumented with fiber Bragg gratings are detailed next, illustrating the special precautions to be taken, and the results obtained.

6.1 Stiffened Panels with Embedded Fiber Bragg Gratings

Three stiffened panels with co-cured stiffener webs were manufactured by means of manual lay-up and autoclave curing. This structure could simulate a portion of the skin panel of a tail plane or a wing of a small aircraft. Two of the panels (panels number 1 and 2) were instrumented with optical fiber Bragg grating sensors bonded on the stiffeners and back-to-back on the skin surface. The other panel (panel number 3) was provided with two embedded optical fiber sensors in each stiffener. Additionally FBGs and strain gauges were bonded on the stiffener webs and on the skin back to back.

The panels have a dimension of 560 mm x 280 mm with 3 blade stiffeners of 20 x 20 mm cross-section situated in the middle line and at 105 mm on the left and on the right from the middle line. Skin thickness is 1 mm and stiffener thickness 1,6 mm. Fiber lay up of the panels has been optimized, being in panel 3 skin: $(\pm 45^{\circ}_{(f)}, \pm 45^{\circ}_{(f)}, 0^{\circ}, \pm 45^{\circ}_{(f)}, \pm 45^{\circ}_{(f)})$ and in the stiffener: $(\pm 45^{\circ}_{(f)}, 0^{\circ}, 0/90^{\circ}_{(f)}, 0^{\circ})$s using a combination of unidirectional and fabric $_{(f)}$ carbon fibers.

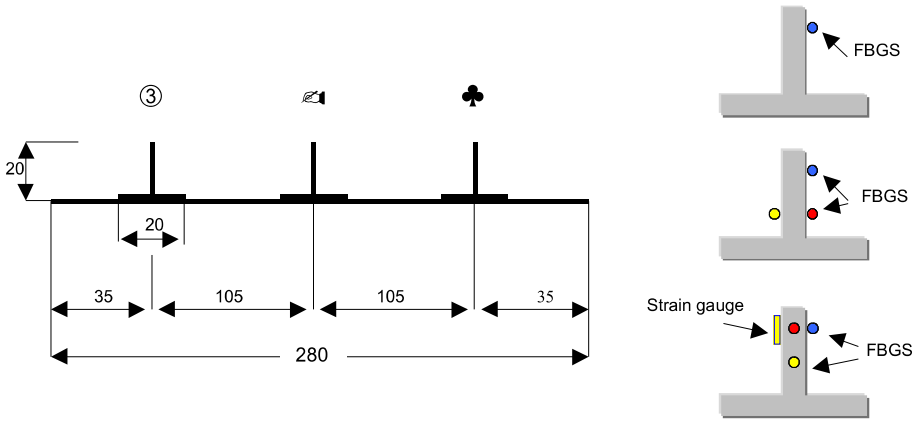

Figure 22: Dimensions of the panels with details of the sensors position.

For manufacturing the stiffened panels a toughened epoxy prepreg material HEXCEL A-193-P/8552S carbon fabric and AS4/8552 unidirectional tape with AS4 high-strength carbon fiber were employed.

The panels were manually laid-up over a reinforced elastomeric mould made of AIRPAD polyacrylic rubber. The elastomeric mould turned out to be very suitable for embedding the optical fibers in the laminate. The elastic rubber surface of the mould enables the optical fibers covered by their protection tubes to be guided between the laminate and the mould and protects them from high-pressure concentrations. The applied curing cycle was the standard one recommended by the prepreg manufacturer (180ºC/ 6bar, 2h). For panel 3 a lower pressure of 4 bars was applied. Panel edges were machined with a diamond disc saw. After edge machining, panel edges were potted into an epoxy/gypsum mixture inside a normalized U-transverse section steel profile (80mm width, 45mm high) to ensure uniform loading (fig. 23).

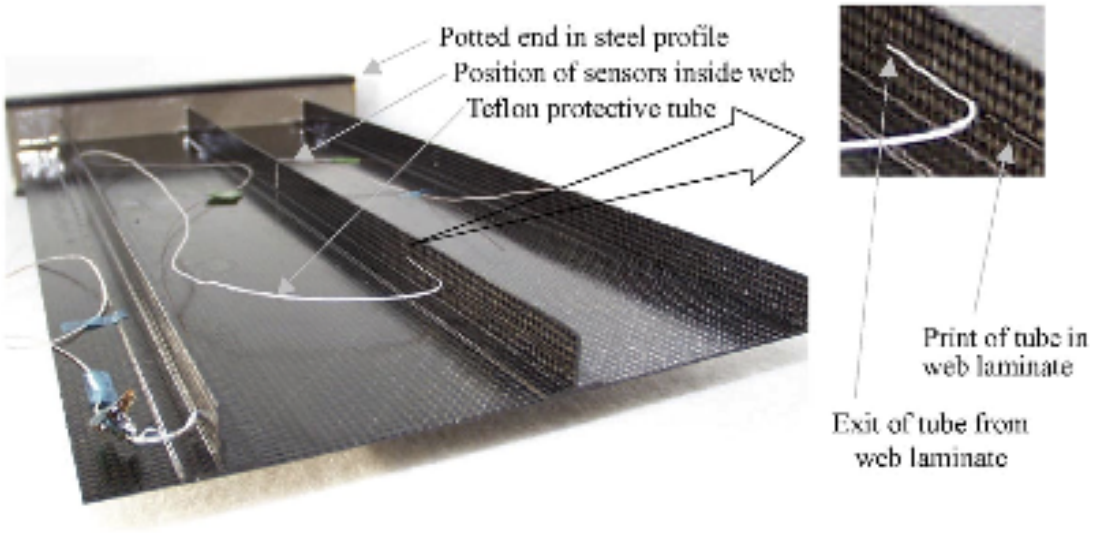

Figure 23: Stiffened composite plate with embedded FBGs.

In panel 3 a 165mm long photosensitive fiber was spliced with an 800mm long single-mode conventional optical fiber. Two FBGs were embedded in the web of each one of the three stiffeners of the panel. The optical fibers were placed between the two central 0º layers and parallel to the reinforcement fibers. Their sensing zone was located at mid-span of the stiffener. Embedding the optical fibers between 0º prepreg layers ensures that they will not be destroyed during the consolidation process and that they will provide a reliable sensor signal that will not be spoiled by the lobed curve surface of the fabric layers. A tiny hole was made passing through the laminate to enable the optical fiber to get out of it. A 0.8mm diameter PTFE tube was used to protect and guide the two optical fibers in each web out of the laminate. This tube was sealed with silicone to prevent resin contamination. A lead of about 25mm of this PTFE tube was left inside the laminate to guaranty a good protection of the fiber at the point where it comes out from the laminate. The rest of this PTFE tube was guided between the laminate and the mould coming out of the mould at its front side. A long portion of the protected optical fiber was left outside the laminate and a connector was fixed to it after curing.

Additional FBGs and conventional strain gauges were surface bonded with cyanoacrylate adhesive on panel 3 to verify the strain measurements of the embedded FBGs, as it was done on panel 1 and 2. Conventional strain gauges were also bonded on the skin to determine the skin buckling. The strain gauges were bonded in all the webs on the left web site at the same location than the upper embedded FBGs; FBGs were bonded on the right web side. In the middle web also additional gauges were bonded in front of the lower FBGs on both sides of the web. All the sensors survived the manufacturing of the part, showing clearly defined spectral peaks with no significant distortion due to complex local strain fields caused by residual stresses.

To verify the exact geometrical position of the embedded optical fibers inside the stiffener webs several X-ray images have been taken from panel 3. The images showing 300 mm of the stiffener length including the fiber egress. A micro focus X-ray system has been used operating at a low voltage level to obtain sufficient high resolution that enables the detection of the small optical fiber inside the composite. Figure 24 shows the X-ray image of stiffener web 3. The two optical fibers can be clearly identified within the composite. On the left side the fiber egress with the protective Teflon tube can be seen. The resolution is high enough to detect not only the fiber path but also possible optical fiber cracking within the composite.

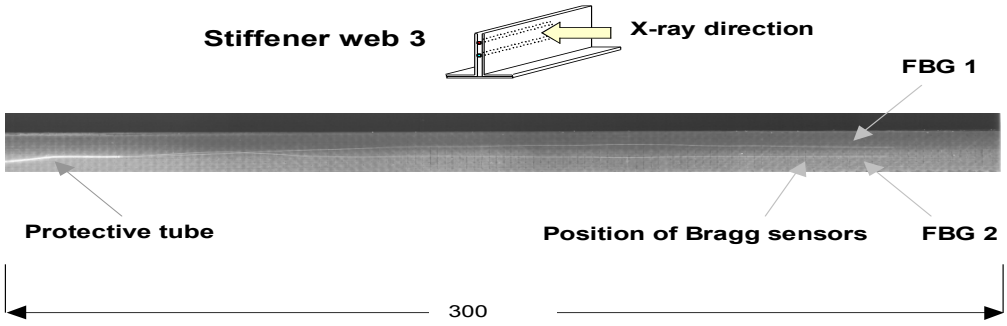

Figure 24: X-ray image of stiffener web 3 in panel 3 indicating the position of the optical fibers and the protective tube at fiber ingress.

Compression tests at room temperature were conducted for the three panels For panels 1 and 2 the sensors worked correctly up to the panel failure. In the explosive rupture the splice of the photosensitive and the conventional single-mode fiber broke at almost every sensor.

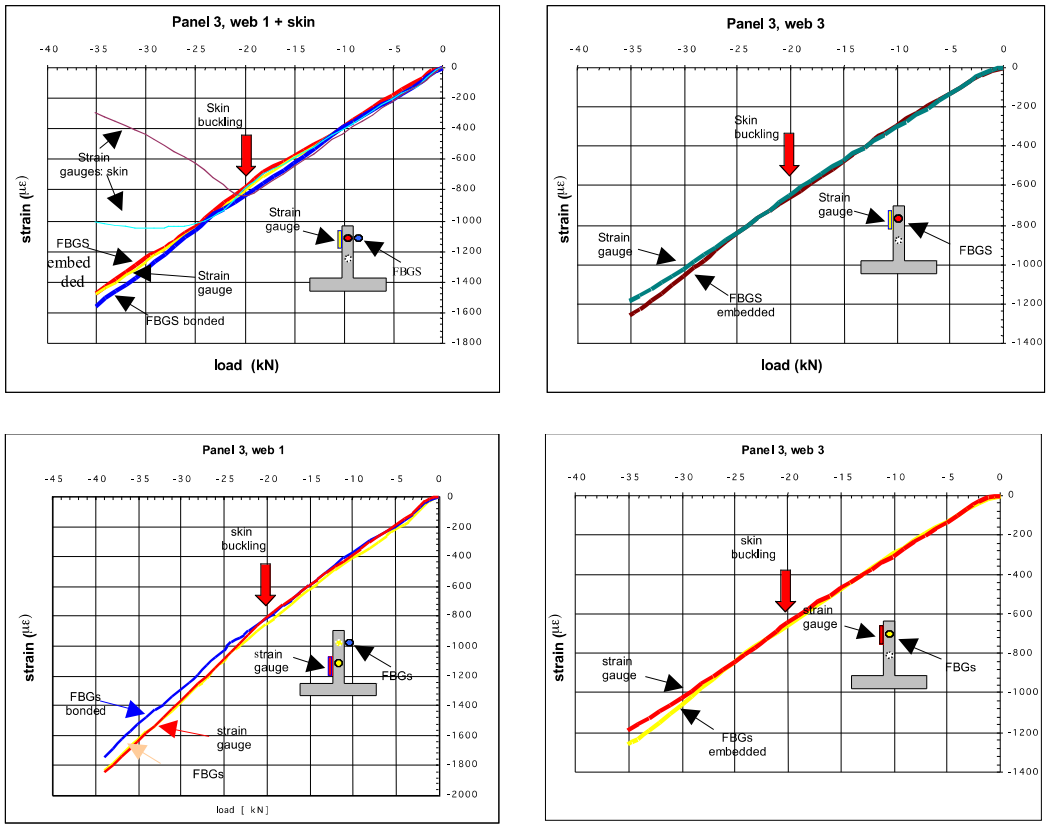

Figure 25: Strain vs. load values from the FBGs and strain gauges of stiffener web.

In the case of panel 3 the six FBGs were embedded in the centerline of the stiffener web so that they were able to measure tensile/compression strains but not transversal bending or twisting of the web. At the beginning of the compression test all the sensors detect the same compressive strain up to the moment when buckling occurs at a strain level of 800 με. A large bending strain in the skin can be noticed by the bifurcation of the sensor signals of the bonded strain gauges. Skin buckling increases the load that has to be carried by the stiffeners and induces also a twisting and transverse bending of the stiffeners. With increasing

load, longitudinal bending of the web occurs. Figure 25 shows the strain measured with the upper embedded FBGs, the bonded FBGs and the bonded strain gauge of the stiffener web 1,2 and 3. The measurement of the skin bonded strain gauges is also included in the graph to indicate the skin buckling.

7.0 CONCLUSIONS

The technology of fiber optic sensors, and particularly of the fibre Bragg gratings, is well matured for strain monitoring and can be used in conventional and advanced structures. It offers several important advantages over conventional electrical strain sensing, namely:

Low size and weight, embeddable capability, single ended cabling.

Long term stability, it can be used for load monitoring during the whole structural life.

Inherent multiplexability, typical 10 sensors/fibre without decreasing reading speed.

Immune to electromagnetic noise, able to work in harsh or explosive environment.

With a perspective of 30 years, three main milestones may be identified in this technology:

a) Discovery of the photosensitivity of the optical fibres by Ken Hill in 1978; first FBGs were engraved by the phase mask procedure in 1989, allowing mass production.

b) Around year 2000, commercial systems for interrogating the FBG were available. Also, first in-flight demonstrations were done.

c) In 1998, NASA wrote a patent (US 5798521) on the multiplexing approach based on the OFDR. We start to see now the first applications and commercial equipments, that may significantly change the instrumentation of structural tests.

Current efforts address either to applications under extreme conditions, like monitoring composites under fire degradation, or to development and demonstration of large sensor arrays, affording a detailed map of the strain field in a complex structure, such as a ship, an aircraft or a bridge. This require new optoelectronics and signal processing systems, able to handling at high speed the information coming from several hundreds of sensing points, compressing this information to the significant events. This is needed if damage detection is intended, because in continuous structures a local damage will produce a very small change in the global strain field. It has to be emphasized that there are not ‘damage sensors’, and probably there will never be. Information about occurrence of structural damage have to be inferred indirectly from other measurements, in this case, strain information.

8.0 BIBLIOGRAPHY

1. B. E. A. Saleh y M. C. Teich. *Fundamental of Photonics*. Wiley Interscience, 1991.

2. J.M. Lopez-Higuera, ed., ‘Handbook of Optical fibre Sensing Technology’ John Wiley and Sons, 2002.

3. Measures, R.M. Structural Monitoring with Fiber Optic Technology, 1st ed.; Academic Press: London, UK, 2004.

4. F. Rodríguez-Lence, P. Muñoz-Esquer, J. M. Menéndez, C. Pardo de Vera, S. Díaz, J. A. Güemes. Smart sensors for resin flow and composite cure monitoring. *Proceedings of the 12th International Conference on Composite Materials, ICCM-12*, Paris, France, 1999.

5. Güemes, S. Díaz-Carrillo, J. M. Menéndez, C. Pardo de Vera, P. Vionis, R. Scherer, D. Bercebal, A. Cuerva. Strain and damage monitoring of wind turbine blades by piezoelectrics and fiber optic sensors. *Proceedings of the ECCM-8 European Conference on Composite Materials*, vol. 3, pp. 357-364, Naples, Italy, 1998.

6. M. Frövel, J.M. Pintado, A. Güemes, E. del Olmo, A. Obst., Multiplexable fiber Bragg grating temperature sensors embedded in CFRP structures for cryogenic applications. *Third European Workshop on Structural Health Monitoring* Destech Publications Inc ISBN 1-932078-63-O pages 938-947. Granada (Spain) 2006.

7. M. Leblanc, S. Y. Huang, M. M. Ohn, A. Güemes, and A. Othonos, Distributed strain measurement based on a fiber Bragg grating and its reflection spectrum analysis. *Optical Letters*, vol. 21, n. 17, pp. 1405-1407, 1996.

8. Güemes, S. Díaz-Carrillo, J. M. Menéndez, Measurement of strain distribution in bonded joints by fiber Bragg Gratings. *Smart Structures and Materials; Proceedings of the Meeting, SPIE-3330*, p. 264-271, San Diego, CA, 1998.

9. A.Güemes, A. Fernandez-Lopez, C. Dominguez, C. de Miguel. Experimental determination of strain inhomogeneities in woven laminates by FBG. *Proceedings of the Intl. Conf. on Composite Materials,* Edinburg (UK) 2009.

10. R. M. Measures, Smart structures with nerves of glass, *Progress on Aerospace Science*, vol. 26, n. 4, pp. 289-351, 1989.

11. J. M. Menéndez, J. A. Güemes, Strain measurements inside thick CFRP laminates at the vicinity of bolted joints. *Smart Structures and Materials; Proceedings of the Meeting, SPIE-3670*, pp. 184-194, Newport, CA. 1999.

12. J. M. Menéndez, and J. A. Güemes. Bragg-grating-based multiaxial strain sensing: its application to residual strain measurement in composite laminates. *Smart Structures and Materials 2000; Proceedings of the Meeting, SPIE-3986*, p. 271-281, Newport, CA, Jun. 2000.

13. M. Frövel, I. Fernandez, J. M. Pintado, J. A. Güemes, J. M. Menéndez, Monitoring the buckling and postbuckling behaviour of stiffened CFRP panels with fibre optic sensors. *European COST F3 Conference on System Identification & Structural Health Monitoring, Proceedings of the Conference*, p. 539-548, Madrid, Spain, Jun. 2000.

14. Mrad, N. Potential of Bragg grating sensors for aircraft health monitoring. Trans. CSME 2007, 31,1-17.

15. Glisic, B.; Inaudi. D. Fibre Optic Methods for Structural Health Monitoring, 1st ed.; John Wiley& Sons, Ltd.: Southern Gate, Chichester, UK, 2007.

16. Culshaw, B.; Kersey, A. Fiber-optic sensing: A historical perspective. IEEE/OSA J. Lightwave Tech.2008, 26, 1064-1078.

17. Connolly, C. Fibre-optic-based sensors bring new capabilities to structural monitoring. Sensors Rev.2006, 26, 236-243.

18. Todd, M.D.; Nichols, J.M.; Trickey, S.T.; Seaver, M.; Nichols, C.J.; Virgin, L.N. Bragg grating-based fibre optic sensors in structural health monitoring. Phil. Trans. Roy. Soc. A 2007.

19. A. Güemes A., Menendez JM, Chapter 3 "Fiber-optics sensors" in 'Structural Health Monitoring' (Eds: Balageas D , Fritzen CP, Güemes A), ISTE, Wiley (2006).

20. Menendez, JM, Güemes, JA "Bragg grating-based multiaxial strain sensing: its application to residual strain measurement in composite laminates" Smart Structures and Materials 2000. San Diego SPIE 3986 (2000).

21. Zhou, G, Sim, L M "Damage detection and assessment in fibre-reinforced composite structures with embedded fibre optic sensors – review" Smart Materials and Structures. Vol. 11, no. 6, pp. 925-939. Dec. 2002.

22. Güemes, J A, Menendez, J M, Frovel, M, Fernandez, I, Pintado, J M "Experimental analysis of buckling in aircraft skin panels by fibre optic sensors" Smart Materials and Structures Vol. 10, no. 3, pp. 490-496. June 2001.

23. C. E. Garcia-Gonzalez, A. Güemes, A. Fernandez-Lopez. High Sampling Rate Fiber-Optic Extensometry for Ultrasonic Wave Detection. 8th International Workshop on Structural Health Monitoring, Stanford, CA (2011).

24. A. Güemes, C. E. Garcia-Gonzalez, I. Gonzalez-Requena, C. de Miguel-Giraldo. *Monitoring the Degradation by Fire of Composite Laminates by Embedded FBG Sensors.* 8th International Workshop on Structural Health Monitoring, Stanford, CA (2011).